Letter

Data driven approach for the measurement of $^{10}Be/^{9}Be$ in cosmic rays with magnetic spectrometers

Francesco Nozzoli* and Cinzia Cernetti

INFN-TIFPA and Trento University, via Sommarive 14 I-38123 Trento, Italy

(Received 26 December 2020; accepted 16 April 2021; published 19 May 2021)

Cosmic rays (CRs) are a powerful tool for the investigation of the structure of the magnetic fields in the galactic halo and the properties of the interstellar medium. Two parameters of the CR propagation model—the galactic halo (half-)thickness H and the diffusion coefficient D—are loosely constrained by current CR flux measurements; in particular, a large degeneracy exists being only H/D well measured. The $^{10}Be/^{9}Be$ isotopic flux ratio (thanks to the 2 My lifetime of ^{10}Be) can be used as a radioactive clock, providing the measurement of CR residence time in the galaxy. This is an important tool for solving the H/D degeneracy. Past measurements of the $^{10}Be/^{9}Be$ isotopic flux ratio in CRs are scarce, limited to low energy, and affected by large uncertainties. Here, a new technique to measure the $^{10}Be/^{9}Be$ isotopic flux ratio with a *data-driven* approach in magnetic spectrometers is presented. The analysis with the data driven approach of beryllium events collected by the PAMELA experiment is shown as an example. It is possible to measure the $^{10}Be/^{9}Be$ flux ratio avoiding the uncertainties related to the Monte Carlo simulation.

DOI: 10.1103/PhysRevD.103.L101101

I. INTRODUCTION

Cosmic rays (CRs) are a powerful tool for the investigation of exotic physics/astrophysics: high-energy CR composition provides information on the mysterious galactic PeVatrons, and the small antimatter component in CRs could reveal dark matter annihilations in our Galaxy.

Besides that, the structure of the magnetic fields in the galactic halo and the properties of the interstellar medium can also be probed by detailed CR flux measurements. In particular, the ratio of secondary CRs (as Li, Be, or B) over the primary CRs (as He, C, or O) is able to provide the *grammage*, that is, the amount of material crossed by CRs in their journey through the Galaxy.

Two parameters of the CR propagation models—the galactic halo (half-)thickness H and the diffusion coefficient D—are loosely constrained by such a *grammage* measurement; in particular, a large degeneracy exists being only H/D well measured [1].

The uncertainties on D and H (this last one is known to be in the range 3–8 kpc) also reflects the accuracy of the determination of secondary antiproton and positrons fluxes that are the background for dark matter or exotic (astro) physics searches [2–4].

The abundances of long-living unstable isotopes in CRs can be used as a radioactive clock, providing a measurement of the CRs residence time in the Galaxy. This time information is complementary to the crossed *grammage*, and thus the abundance of radioactive isotopes in CRs is an important tool for solving the existing H/D degeneracy in CR propagation models.

A. Be isotopic measurements in cosmic rays

Only a few elements in cosmic rays (Be, Al, Cl, Mg, and Fe) contain long-living radioactive isotopes, with beryllium being the lightest, i.e., the most promising for a measurement of isotopic composition in the relativistic kinetic energy range. Three beryllium isotopes are found in cosmic rays.

1. ^{7}Be: stable as a bare nucleus in CRs. On Earth it decays by electron capture ($T_{1/2} = 53$ days).
2. ^{9}Be: stable.
3. ^{10}Be β-radioactive nucleus ($T_{1/2} = 1.39 \times 10^{6}$ y).

The missing ^{8}Be has a central role in stellar and big bang nucleosynthesis, as the extremely short half-life (8.19×10^{-17} s) represents a bottleneck for an efficient synthesis of heavier nuclei in the Universe. From the measurement point of view, this "isotopic hole" in the beryllium mass spectrum is very useful to determine the large amount of ^{7}Be and reduce the contamination in the identification of ^{9}Be and ^{10}Be.

The identification of beryllium isotopes in magnetic spectrometers requires the simultaneous measurement of particle rigidity, $R = p/Z$, and velocity, $\beta = v/c$, allowing for a reconstruction of the mass $m = RZ/(\gamma\beta)$.

The mass resolution of magnetic spectrometers onboard past/current CR experiments ($\delta M \simeq 0.4$–1 amu) does not allow for an event-by-event isotope identification; therefore, the "traditional" approach for the measurement of

*Francesco.Nozzoli@cern.ch

beryllium isotopic abundances relies on the comparison of the experimental mass distribution with a Monte Carlo simulation.

This approach requires a very well-tuned Monte Carlo simulation of the experiment, and the possible small residual discrepancies with the real detector response could prevent the measurement of the (interesting) small amount of ^{10}Be.

This systematics was well described in Ref. [5] where the "Monte-Carlo-based" analysis of beryllium events collected by the PAMELA experiment allowed only the measurement of $^{7}\mathrm{Be}/(^{9}\mathrm{Be}+{}^{10}\mathrm{Be})$.

In the following a *data-driven* approach for the measurement of beryllium isotopic abundances with magnetic spectrometers is described, which can evade the systematics related to Monte Carlo simulation. In particular, as an example we apply this new approach to PAMELA beryllium event counts (gathered from Figs. 3 4 of Ref. [5]) and a preliminary measurement of $^{10}\mathrm{Be}/^{9}\mathrm{Be}$ in the 0.2–0.85 GeV/n range is provided. Figure 3 of Ref. [5] contains the number of beryllium events as a function of β measured by the time-of-flight (ToF) subdetector and rigidity measured by the silicon tracker, whereas Fig. 4 of Ref. [5] contains the number of beryllium events as a function of dE/dx measured by the electromagnetic calorimeter and rigidity measured by the silicon tracker. Both figures contain color-coded small integers, and therefore counts can be extracted by image analysis as if they were published in a table.

II. DATA-DRIVEN ANALYSIS

Knowing the true values of beryllium isotope masses and a physically motivated scaling of the mass resolution for the three beryllium isotopes, the shape of the isotope mass distributions can be retrieved, by self-consistency, solely from measured data. In particular, the expected mass resolution for a magnetic spectrometer is

$$\frac{\delta M}{M}=\sqrt{\left(\frac{\delta R}{R}\right)^2+\gamma^4\left(\frac{\delta\beta}{\beta}\right)^2}. \tag{1}$$

Typically the isotopic measurement is pursued in kinetic energy/nucleon bins (i.e., in β bins), and therefore the velocity contribution to mass resolution is constant for the different isotopes. Moreover, in the (low) kinetic energy range accessible by current isotopic measurements, the rigidity resolution is dominated by multiple Coulomb scattering, i.e., $\delta R/R$ is nearly constant for the three different isotopes. Finally, the masses of the three Be isotopes are within 30%, and therefore for a fixed β value the rigidity values for different Be isotopes are within 30%; for this reason, as a good approximation, $\delta M/M$ is constant and we can assume that the three unknown mass distributions (hereafter also called *templates*) have the same relative width.

A. Template transformations

We can define T_7, T_9, and T_{10} as the unknown normalized templates for ^{7}Be, ^{9}Be, and ^{10}Be respectively.

A template T_a can transform into the template T_b by applying the operator $A_{a,b}T_a(x)=T_b(x)$, and we can assume that $A_{a,b}$ is just a transformation of the coordinates $x\to g(x)$; therefore, to ensure template normalization,

$$T_b(x)=A_{a,b}T_a(x)=\frac{dg}{dx}T_a(g(x)). \tag{2}$$

In principle, an infinite set of functions $g(x)$ are able to perform a transformation among two specific templates; however, we are typically interested in monotonic functions to avoid folding the templates. A very simple set of transformations are the linear ones $L_{a,b}$ defined by translation and scale transformations: $x\to mx+q$. The linear $L_{a,b}$ transforms a normal distribution into a normal distribution.

Defining σ_a as the rms of template T_a and x_a as the median of template T_a, the linear transformation $L_{a,b}T_a=T_b$ is the function $x\to\frac{\sigma_a}{\sigma_b}x+[x_a-\frac{\sigma_a}{\sigma_b}x_b]$.

The same transformation but applied to another, different template $L_{a,b}T_c=T_d$ provides $\sigma_d=\sigma_c\frac{\sigma_b}{\sigma_a}$ and $x_d=x_b+(x_c-x_a)\frac{\sigma_b}{\sigma_a}$.

The linear transformation that satisfies the assumption ($\delta M/M=\mathrm{const}$) is simply $x\to\frac{x_a}{x_b}x$, that is, a pure scaling depending only on known beryllium isotope mass ratios and not on the unknown mass resolution or template shapes. In the following, the linear approximation for the template transformation is adopted.

B. Data-driven template evaluation and fit

Defining the known (measured) data distribution $D(x)$ and assuming as fixed the three fractions ^{n}Be/Be, the following system can be considered:

$$\begin{aligned}
D(x)&={}^{7}\mathrm{Be}T_7+{}^{9}\mathrm{Be}T_9+{}^{10}\mathrm{Be}T_{10},\\
L_{7,9}D(x)&={}^{7}\mathrm{Be}T_9+{}^{9}\mathrm{Be}L_{7,9}T_9+{}^{10}\mathrm{Be}L_{7,9}T_{10},\\
L_{7,10}D(x)&={}^{7}\mathrm{Be}T_{10}+{}^{9}\mathrm{Be}L_{7,10}T_9+{}^{10}\mathrm{Be}L_{7,10}T_{10}.
\end{aligned} \tag{3}$$

Therefore, the ^{7}Be template can be written as

$$\begin{aligned}
T_7=\frac{1}{{}^{7}\mathrm{Be}}\left[D-\frac{{}^{9}\mathrm{Be}}{{}^{7}\mathrm{Be}}L_{7,9}D-\frac{{}^{10}\mathrm{Be}}{{}^{7}\mathrm{Be}}L_{7,10}D\right]+\left(\frac{{}^{9}\mathrm{Be}}{{}^{7}\mathrm{Be}}\right)^2T_{G1}\\
+\frac{{}^{9}\mathrm{Be}}{{}^{7}\mathrm{Be}}\frac{{}^{10}\mathrm{Be}}{{}^{7}\mathrm{Be}}(T_{G2}+T_{G3})+\left(\frac{{}^{10}\mathrm{Be}}{{}^{7}\mathrm{Be}}\right)^2T_{G4},
\end{aligned} \tag{4}$$

and the last four terms (*ghost* templates) are defined by

$$
\begin{aligned}
T_{G1} &= L_{7,9}T_9 = L_{7,x_{G1}}T_7,\\
T_{G2} &= L_{7,9}T_{10} = L_{7,x_{G2}}T_7,\\
T_{G3} &= L_{7,10}T_9 = L_{7,x_{G3}}T_7,\\
T_{G4} &= L_{7,10}T_{10} = L_{7,x_{G4}}T_7.
\end{aligned} \tag{5}
$$

The median values of the ghost templates can be evaluated as

$$
\begin{aligned}
x_{G1} &= x_9 + (x_9 - x_7)\frac{\sigma_9}{\sigma_7} \simeq 11.5 \text{ amu},\\
x_{G2} &= x_9 + (x_{10} - x_7)\frac{\sigma_9}{\sigma_7} \simeq 13 \text{ amu},\\
x_{G3} &= x_{10} + (x_9 - x_7)\frac{\sigma_{10}}{\sigma_7} \simeq 13 \text{ amu},\\
x_{G4} &= x_{10} + (x_{10} - x_7)\frac{\sigma_{10}}{\sigma_7} \simeq 14 \text{ amu}.
\end{aligned} \tag{6}
$$

Given that the ghost templates are placed beyond T_{10} and that we know $^7\mathrm{Be} > {}^9\mathrm{Be} > {}^{10}\mathrm{Be}$, the contribution of ghost templates in Eq. (4) is small and T_7 can be iteratively evaluated from measured data by using Eq. (5).

Once T_7 is obtained, the other templates are straightforwardly obtained by using $L_{7,9}$ and $L_{7,10}$, and a χ^2 value for the fixed $^7\mathrm{Be}/\mathrm{Be}$ and $^9\mathrm{Be}/{}^{10}\mathrm{Be}$ is obtained by comparison with $D(x)$.

This data-driven approach has been tested on the Monte Carlo simulated events for beryllium isotopes in the AMS-02 spectrometer [6] and it is able to correctly retrieve the injected isotopic ratios within statistical fluctuations. In the following, as an example we apply this approach to Be events published by the PAMELA experiment [5].

In Fig. 1, the χ^2 value for the configurations defined by $^7\mathrm{Be}/\mathrm{Be}$ and $^{10}\mathrm{Be}/{}^9\mathrm{Be}$ parameters is shown for the example of PAMELA-ToF events in the 0.65–0.85 GeV/n range (last bin of our analysis). The best fit is marked by a red triangle and the 68% confidence interval is surrounded by a red contour.

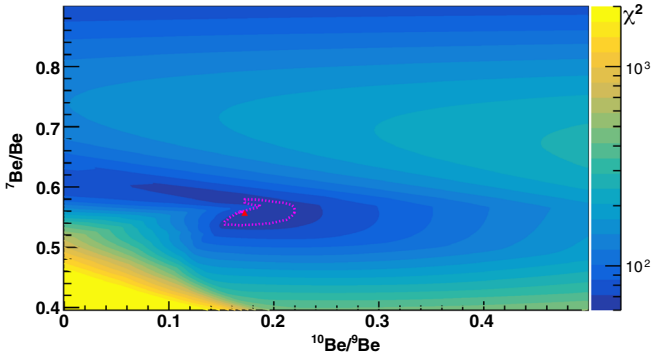

FIG. 1. Map of χ^2 configurations for PAMELA-ToF in the 0.65–0.85 GeV/n region. The best fit is marked by a red triangle and the 68% confidence interval is surrounded by a red contour.

It is important to note that three naive solutions of the data-driven analysis are obviously $^7\mathrm{Be}/\mathrm{Be} = 1$, $^9\mathrm{Be}/\mathrm{Be} = 1$, and $^{10}\mathrm{Be}/\mathrm{Be} = 1$, and these naive solutions are characterized by $\chi^2 = 0$. Therefore, the evaluation of the confidence interval for the physical solution requires some care; in particular, the statistical bootstrap [7] was adopted to evaluate confidence intervals for this example.

In Fig. 2 the best fit for the example of the PAMELA-ToF 0.65–0.85 GeV/n region is shown. The templates are obtained with this data-driven approach.

Figure 2 also shows the same data and templates but as a function of $|M - 10|$.

It is important to note that under the assumption of a constant relative mass resolution ($\delta\mathrm{M}/\mathrm{M} = \text{const.}$) the Eq. (4) is scale invariant. For this reason the results obtained by data-driven analysis are quite solid regarding possible rigidity/velocity scale miscalibrations that could prevent the *traditional* Monte Carlo based analysis, as shown in Ref. [5]. As a practical example, we also apply the data-driven analysis to events measured by the PAMELA calorimeter (Fig. 4 of ref. [5]) even without a tuned Monte Carlo model/calibration for the dE/dx measurement.

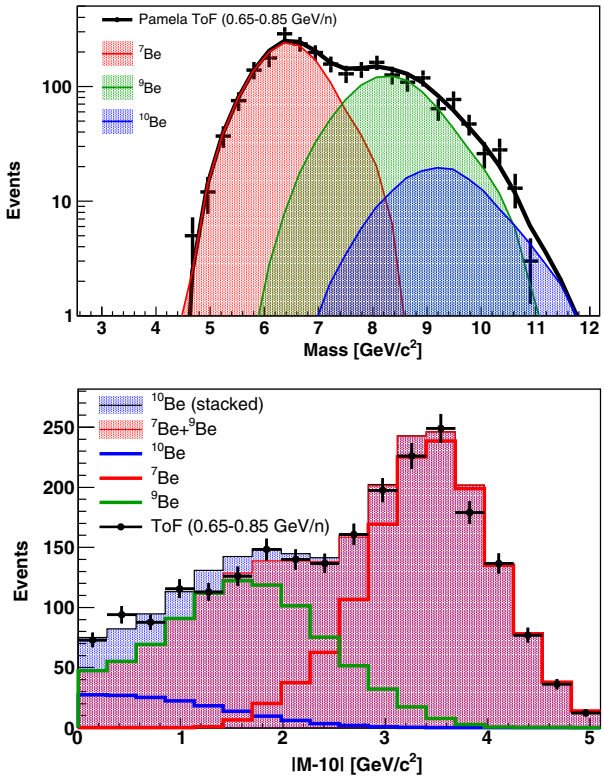

FIG. 2. Example of beryllium isotope measurements with the data-driven analysis of PAMELA-ToF data collected in the 0.65–0.85 GeV/n range. The black continuous line is the sum of the three beryllium components. In the bottom plot the same data are shown as a function of $|M - 10|$, which allows to stack the $^{10}\mathrm{Be}$ contribution (blue filled) onto the $^7\mathrm{Be} + {}^9\mathrm{Be}$ contribution (red filled).

III. RESULTS AND DISCUSSION

The results of the data-driven analysis of ^{7}Be/Be and ^{10}Be/^{9}Be ratios using the PAMELA data [5] are shown in Fig. 3 and compared with previous measurements [8–19].

The data-driven measurement obtained with PAMELA-ToF (black dots) is in reasonable agreement with the one obtained with the PAMELA calorimeter (blue square) and, regarding ^{7}Be/Be, the results of the data-driven analysis are in agreement with those published in Ref. [5] based on the Monte Carlo template fit of the PAMELA data (orange dots). The green shaded regions in Fig. 3 are a cautious estimation of the systematic error for the data-driven analysis, related to the possible departures from the assumption of pure template scaling, i.e., considering $\delta M/M = K(1 \pm \alpha_M)$ where K is a constant and α_M is a possible, small, isotope-dependent correction. In particular, knowing the measured PAMELA rigidity resolution [20] in the considered 1.5–4 GV range and knowing that, for a fixed velocity, the rigidity of ^{7}Be is 70% of the rigidity of ^{10}Be, a cautious upper limit of $\alpha_M < 10\%$ can be inferred for the possible departures from the exact template scaling relation.

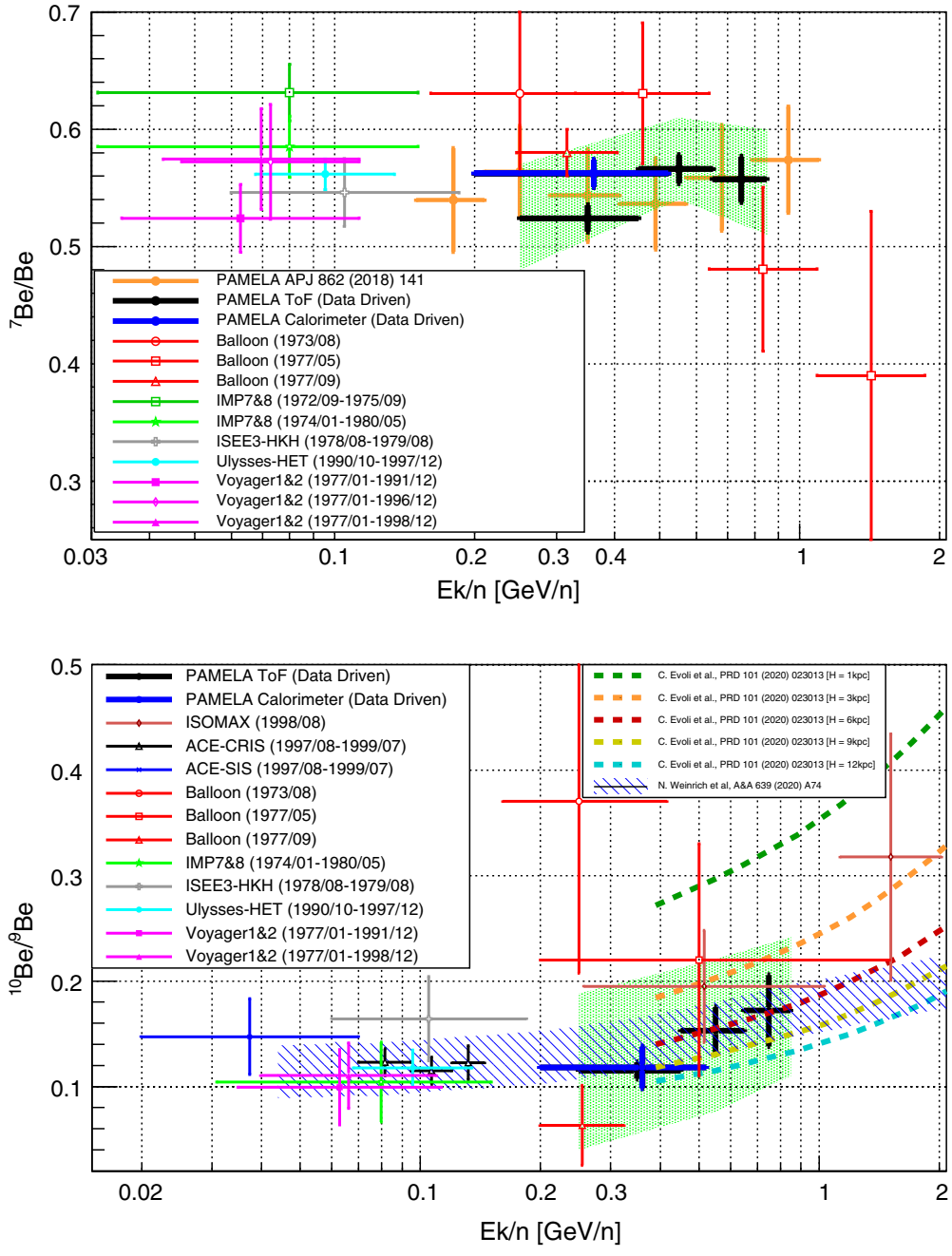

FIG. 3. Comparison of the results of the data-driven analysis for the ^{10}Be/^{9}Be and ^{7}Be/Be fractions with previous experiments and with a Monte Carlo based analysis. Green shaded contours are the systematic uncertainties inferred for the data-driven analysis.

A complete evaluation of systematic uncertainties also requires a study of the possible differences in the selection acceptance for ^{7}Be, ^{9}Be, and ^{10}Be and the different contaminations due to B, C, N, and O fragmentations crossing the material above the detector. These systematics cannot be estimated without a Monte Carlo simulation of the detector; however, the contribution is expected to be small (few %) with respect to the wide uncertainties plotted in Fig. 3 [21].

In conclusion, the new information provided by the data-driven analysis, when applied to PAMELA data, is a relatively precise estimation of the ^{10}Be/^{9}Be ratio in the range 0.2–0.85 GeV/n where existing measurements are scarce and affected by large uncertainty. In particular, it is interesting to note that this measurement strengthens the previous indications for a rising ^{10}Be/^{9}Be ratio at large kinetic energy and is in good agreement with the models of Refs. [2,3] that are recent predictions of ^{10}Be/^{9}Be tuned with the up-to-date AMS-02 fluxes (and previous ^{10}Be/^{9}Be measurements).

[1] C. Evoli, G. Morlino, P. Blasi, and R. Aloisio, AMS-02 beryllium data and its implication for cosmic ray transport, Phys. Rev. D **101**, 023013 (2020).

[2] J. Feng, N. Tomassetti, and A. Oliva, Bayesian analysis of spatial-dependent cosmic-ray propagation: Astrophysical background of antiprotons and positrons, Phys. Rev. D **94**, 123007 (2016).

[3] N. Weinrich, M. Boudaud, L. Derome, Y. Génolini, J. Lavalle, D. Maurin, P. Salati, P. Serpico, and G. Weymann-Despres, Galactic halo size in the light of recent AMS-02 data, Astron. Astrophys. **639**, A74 (2020).

[4] M. Korsmeier and A. Cuoco, Galactic cosmic-ray propagation in the light of AMS-02: Analysis of protons, helium, and antiprotons, Phys. Rev. D **94**, 123019 (2016).

[5] W. Menn *et al.*, Lithium and beryllium isotopes with the PAMELA experiment, Astrophys. J. **862**, 141 (2018).

[6] M. Aguilar *et al.* (AMS Collaboration), Properties of Cosmic Helium Isotopes Measured by the Alpha Magnetic Spectrometer, Phys. Rev. Lett. **123**, 181102 (2019).

[7] B. Efron, Better bootstrap confidence intervals, J. Am. Stat. Assoc. **82**, 171 (1987).

[8] N. E. Yanasak, M. E. Wiedenbeck, R. A. Mewaldt, A. J. Davis, A. C. Cummings, J. S. George, R. A. Leske, E. C. Stone, E. R. Christian, T. T. von Rosenvinge, W. R. Binns, P. L. Hink, and M. H. Israel, Measurement of the secondary radionuclides ^{10}Be, ^{26}Al, ^{36}Cl, ^{54}Mn, and ^{14}C and implications for the galactic cosmic-ray age, Astrophys. J. **563**, 768 (2001).

[9] F. A. Hagen, A. J. Fisher, and J. F. Ormes, Be-10 abundance and the age of cosmic rays—A balloon measurement, Astrophys. J. **212**, 262 (1977).

[10] A. Buffington, C. D. Orth, and T. S. Mast, A measurement of cosmic-ray beryllium isotopes from 200 to 1500 MeV per nucleon, Astrophys. J. **226**, 355 (1978).

[11] W. R. Webber and J. Kish, Further studies of the isotopic composition of cosmic ray li, BE and B nuclei—Implications for the cosmic ray age, in *ICRC* (1979), Vol. 1, p. 389, https://ui.adsabs.harvard.edu/abs/1979ICRC....1..389W.

[12] M. Garcia-Munoz, G. M. Mason, and J. A. Simpson, The age of the galactic cosmic rays derived from the abundance of Be-10, Astrophys. J. **217**, 859 (1977).

[13] M. Garcia-Munoz, J. A. Simpson, and J. P. Wefel, The propagation lifetime of galactic cosmic rays determined from the measurement of the beryllium isotopes, in *ICRC* (1981), Vol. 2, pp. 72–75, https://ui.adsabs.harvard.edu/abs/1981ICRC....2...72G.

[14] M. E. Wiedenbeck and D. E. Greiner, A cosmic-ray age based on the abundance of Be-10, Astrophys. J. Lett. **239**, L139 (1980), http://adsabs.harvard.edu/full/1980ApJ...239L.139W.

[15] T. Hams, L. M. Barbier, M. Bremerich, E. R. Christian, G. A. de Nolfo, S. Geier, H. Göbel, S. K. Gupta, M. Hof, W. Menn, R. A. Mewaldt, J. W. Mitchell, S. M. Schindler, M. Simon, and R. E. Streitmatter, Measurement of the abundance of radioactive ^{10}Be and other light isotopes in cosmic radiation up to 2 GeV nucleon^{-1} with the balloon-borne instrument ISOMAX, Astrophys. J. **611**, 892 (2004).

[16] J. J. Connell, Galactic cosmic-ray confinement time: ULYSSES high energy telescope measurements of the secondary radionuclide 10Be, Astrophys. J. Lett. **501**, L59 (1998).

[17] A. Lukasiak, P. Ferrando, F. B. McDonald, and W. R. Webber, The isotopic composition of cosmic-ray beryllium and its implication for the cosmic ray's age, Astrophys. J. **423**, 426 (1994).

[18] A. Lukasiak, F. B. McDonald, and W. R. Webber, Voyager measurements of the isotopic composition of Li, Be and B nuclei, in *ICRC* (1997), Vol. 3, p. 389, https://ui.adsabs.harvard.edu/abs/1997ICRC....3..389L.

[19] A. Lukasiak, Voyager measurements of the charge and isotopic composition of cosmic ray Li, Be and B nuclei and implications for their production in the galaxy, in *ICRC* (1999), Vol. 3, p. 41, https://ui.adsabs.harvard.edu/abs/1999ICRC....3...41L.

[20] S. Straulino *et al.* (PAMELA Collaboration), The PAMELA silicon tracker, Nucl. Instrum. Methods Phys. Res., Sect. A **530**, 168 (2004).

[21] It is important to note that this preliminary measurement is shown as an example of application of the data-driven method. A full data analysis using this approach by the PAMELA-collaboration could provide the complete measurement of ^{10}Be/^{9}Be up to 1 GeV/n.